Physica A 391 (2012) 5727–5738

Contents lists available at SciVerse ScienceDirect

Physica A

journal homepage: www.elsevier.com/locate/physa

Earthquake model describes traffic jams caused by imperfect driving styles

Ferenc Járai-Szabó *, Zoltán Néda

Department of Physics, Babes-Bolyai University, str. Kogalniceanu 1, RO-400084 Cluj-Napoca, Romania

ARTICLE INFO

Article history:
Received 19 January 2012
Received in revised form 8 April 2012
Available online 19 June 2012

Keywords:
Highway traffic
Disorder induced phase transition
Spring-block models

ABSTRACT

The wide modeling potential of the classical spring-block type system is illustrated by an interdisciplinary application. A simple one-dimensional spring-block chain with asymmetric spring forces is used to model idealized single-lane highway traffic and the emergence of phantom traffic jams. Based on the stop-time statistics of one car in the row, a proper order parameter is defined. By extensive computer simulations the parameter space of the model is explored, analyzed and interpreted. Existence of free and congested flow phases is confirmed and the transition between them is analyzed.

1. Introduction

Almost half a decade elapsed since the first application of the spring-block system as an interdisciplinary modeling tool. In their classic paper Burridge and Knopoff [1] showed that a simple chain of blocks interconnected by springs and sliding on a frictional substrate is appropriate for understanding the famous Gutenberg–Richter scaling law [2] regarding the distribution of earthquakes by their magnitude. Due to the simplicity of the spring-block model collective phenomena from widely different fields have been explored by using this simple and intuitive approach. As a result, a whole family of models has been developed by modifying either the tension of the spring forces or the interconnection topology, and resulting in successful applications in widely different fields. For a brief review on spring-block models and their applications we recommend the recent work of Mate et al. [3] and the references within.

Here, we show that this simple model can be applied also for understanding some elements of accident free, one-lane traffic. Being aware that many models exist for describing this apparently simple but in reality complex phenomenon, our aim is not to give an even more sophisticated model leading to a more realistic description. This is always possible by refining the existing models and by introducing new parameters. Instead, we plan to show that the classical spring-block chain with asymmetric interactions can capture many important aspects of this everyday-life phenomenon and by this our aim is to prove once again the modeling power of this simple system.

The rapid growth of vehicle numbers during the last century caused an increased complexity in our road traffic and transportation systems. Unfortunately, in such conditions, traffic congestion becomes an everyday problem for drivers. The variety of complex non-linear phenomena present in such agglomerated traffic systems has attracted the attention of a large number of researchers (for a review please consult the recent work of Nagatani [4], or the interdisciplinary review by Helbing [5]). Accordingly, since the early 1930s many empirical data on different highways have been collected [6–8]. In the meantime traffic data collection systems have substantially evolved as well [9,10]. On the theoretical side, many different models have been developed [11,5,12,13]. From the conceptual point of view the models are usually classified as microscopic and macroscopic models. With respect to the mathematical representation these models are categorized as car-following and cellular automata models. Moreover, there are some non-traditional models that have both microscopic

* Corresponding author.
E-mail address: jferenc@phys.ubbcluj.ro (F. Járai-Szabó).

0378-4371/$ – see front matter © 2012 Elsevier B.V. All rights reserved.
doi:10.1016/j.physa.2012.06.037

and macroscopic aspects as well. These models form the category of mesoscopic models. One recent example of a stochastic mesoscopic model could be the probabilistic traffic flow theory [14] that includes the nonlinear effects of small perturbations. It was also shown [15] that finite reaction times are essential factors of driver behavior that affects the performance and stability of traffic. Despite many existing studies in the field, the phenomenon of spontaneous traffic jam formation is not completely understood.

The simplest, but already quite complex form of the traffic is the accident-free and single-lane motion of a chain of cars. The motion of the queue in this simple form of traffic is primarily governed by the leading car and the statistics of driving attitudes. From empirical observations we know that this kind of traffic can be either "free" with a continuous flow structure or congested with a stop-and-go motion of cars. The congested traffic usually appears if the leading car is moving slowly and the differences between the driving attitudes of drivers are substantial. In such situations the car row will evolve non-continuously in avalanches of widely different sizes, and a sequence of jams of different magnitudes will appear and propagate backward through the system. This form of traffic is also known as a shockwave traffic jam or 'phantom traffic jam'. A systematic analysis of empirical traffic states of a 30 km long section of the German freeway A5 near Frankfurt [16,17] reported a rich variety of congested traffic states, interpreted as the spatial coexistence of altogether six different traffic states.

"Why do traffic jams appear on highways?" — is the natural question asked by the authors of the first experimental article that investigates the spontaneous shockwave traffic jam formation [18,19]. By a planned experiment performed on a circuit they show that the emergence of a traffic jam may occur even in the absence of a bottleneck. If one looks at their experiments (i.e. their video recording posted on youtube [20]) it is immediately observable that at the initial stage, vehicles are running continuously each with the same velocity, but roughly 10 min later a first shockwave traffic jam emerges spontaneously and propagates in the system. Shortly after this experiment these emergent shockwaves have been identified as nonlinear traveling wave solutions called 'jamiton solutions' of the purely deterministic hyperbolic continuum traffic equations [21].

The present work is inspired and motivated by the experiments of Sugiyama et al. Based on their work, the formation of a traffic jam is understood as a collective phenomenon. The simple spring-block system offers usually an excellent and intuitive modeling framework for understanding phenomena where avalanche-like dynamics is observed [22]. Adapting such a model for this problem is quite straightforward. A spring-block chain with asymmetric interactions is considered, where blocks will model the cars and the springs the distance keeping tendency of drivers. The limitations of the model are clearly defined by the forced mechanical analogy: harmonic spring forces governing the acceleration and deceleration of cars; mechanical friction forces modeling reaction times and disorder in driving styles; and applying dynamical laws of classical mechanics for describing a complex time evolution. All this is done for the sake of keeping the spring-block modeling paradigm.

Through large-scale computer simulations the conditions at which our spring-block model system's flow self-organizes into a congested traffic flow phase are identified. Contrary to most of the studies in the field of highway traffic we focus on a measure characteristic for one car (block) in the row: the distribution of time intervals during which the car is not moving. These time intervals will be labeled hereafter as rest times or stop times. Based on the rest time distributions an order parameter will be defined and the parameter space of the model is explored and analyzed. The present model is able to reproduce only two traffic phases: a free flow and a congested flow phase. It is shown that the transition between the free and congested traffic states is realized through a disorder-induced second order phase transition. Based on evident analogies with the model elements, it is concluded that the imperfections in driving styles play an important role in the formation of traffic jams.

The rest of the paper is organized as follows. First, the spring-block model of highway traffic is presented starting from basic ideas that originates from earthquake modeling. The main ingredients, model dynamics and model parameters are discussed as well. Then, in the "Results" section an order parameter is defined and the parameter space of the model is mapped. Finally, in the "Discussion and conclusions" section the experiment of Sugiyama et al. is discussed from the viewpoint of the spring-block model.

2. The spring-block model for highway traffic

The spring-block approach for the single-lane highway traffic was described in detail in our previous work [23]. However, for the sake of completeness a brief review of the model will be included here.

2.1. From earthquakes to traffic modeling

The model used belongs to a model family with broad interdisciplinary applications called spring-block type models introduced in 1967 by Burridge and Knopoff [1]. It consists of simple elements: blocks that can slide with friction on a horizontal plane connected in a lattice-like topology by springs. Later, due to the spectacular development of computers and computational techniques, this simple model proved to be very useful in describing many phenomena in different areas of science. Most of the collective phenomena that occur on a mesoscopic scale in solid materials such as cracking or fragmentation in drying granular materials [24,25], capillarity driven self-organization [26–28] or magnetization processes and Barkhausen noise [22] can be modeled by spring-block type models. The studies mentioned above suggest that spring-block models are useful for those complex phenomena where avalanche-like dynamics, collective behavior or pattern formation is present.

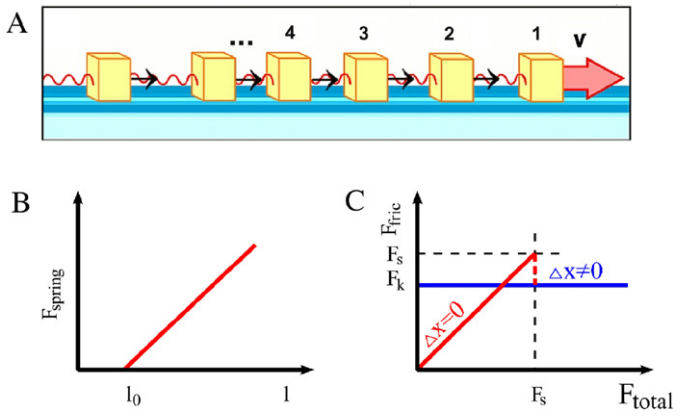

Fig. 1. The spring-block model for highway traffic. The used spring-block chain is shown on panel (A) while the force profile for spring-tension and friction are shown on panels (B) and (C), respectively.

In the spring-block approach the idealized car queue that moves on a single highway lane is modeled as a chain of blocks dragged by the first block that advances with a constant velocity v (as sketched in Fig. 1(A)). Blocks are labeled after their ordinal number in the row so that the externally dragged block (the first in the queue) has label 1 and the last block in the queue is labeled with N. The position of the blocks is denoted by $x^{(i)}$, where $i = \overline{1, N}$.

The blocks are connected by springs of equilibrium length l_0 and spring constant k having the classical force profile shown in Fig. 1(B). The interactions resulting from the springs model the aim of drivers to keep a certain distance from the car ahead. The linearity of the spring force is imposed for the sake of simplicity and in order to keep the analogy with the general spring-block model. In order to be realistic, the springs used cannot be classical mechanical springs with forces acting on both their ends, because in case of accident-free traffic the front car should not be influenced by the car from behind. Therefore, this distance keeping interaction acts only on the car behind. In such a system, the action–reaction principle is violated and, in this sense, it cannot be any longer considered as a realistic mechanical system.

Recently it has been argued that for modeling the drivers' actions, one has to account for their reaction time and velocity adaptation time [29]. In the computational models, one has to account with a numerical update time as well. The last two of these characteristic times will be included in the dynamics of the spring-block model presented later. It has to be noted that in this form, the spring-block model implements instantaneous acceleration responses that correspond to zero reaction times.

Another important ingredient, which can be incorporated in the model, is the disorder generated by the unpredictable reactions of drivers. In order to minimize the ingredients of the model and to keep the analogy with spring-block systems the reaction times of drivers are introduced through friction forces that oppose the sliding of the blocks. These friction forces are generated randomly and independently for each new position of the blocks. As a first approximation we consider for this quantity a normal distribution with a fixed mean $\langle F_s \rangle$ and standard deviation σ. As a result of this both a spatial and a temporal disorder are introduced. Spatial disorder models differences in the driving styles of the drivers while temporal disorder approximates changes in the drivers' reaction times. The mean value of the friction force may be connected to the average reaction time of the drivers. Friction forces that are smaller than the average value correspond to a quicker reaction than the average. Similarly, friction forces bigger than the average describe late reactions. A narrow distribution around a mean is expected for fresh, rested drivers. As the driver gets tired, the driving imperfections are gradually increased corresponding to a broad distribution in the friction forces.

In analogy with real mechanical systems, static and kinetic friction forces are considered. They are denoted by F_s and F_k, respectively. The friction force profile is presented in Fig. 1(C). The selection of the friction force value depends on the previous displacement Δx of the block and the total force F_{total} acting on it. Similarly with classical dynamical systems, the maximum possible value of the static force is considered to be greater than the kinetic one. For simplicity reasons in our model their ratio is kept constant: $f = F_k/F_s$. By this assumption we include in the model the tendency of drivers to react quicker to an event when the car is in motion. In such cases, there is no need to release the brakes and then step on the accelerator pedal and slowly release the clutch as would be the case for a stopped car. This effect, when standing cars accelerate with lower probability than the moving ones is known as the "slow-to-start rule". This rule was first proposed by Barlovic et al. [30] as a simple generalization of the Nagel and Schreckenberg (NaSch) probabilistic cellular automaton models [31].

The simulation follows the typical steps of a simplified molecular dynamics simulation with a properly selected timestep Δt and is summarized below.

- *Simulation step* #1: *calculation of forces acting on each block.* All blocks are visited and the spring force F_{spring} acting on each block i is calculated by

$$F^{(i)}_{spring}(t) = k\left[l^{(i)}(t - \Delta t) - l_0\right], \tag{1}$$

where $l^{(i)}$ denotes the length of the spring connected to the front of the ith block. If the block is at rest (its previous displacement $\Delta x^{(i)}(t-\Delta t)=0$) the spring force is compared to the static friction. If $F^{(i)}_{spring}(t) \leq F^{(i)}_{s}(t)$ the static friction equals the spring force and the total force acting on the block will be

$$F^{(i)}_{t}=0. \tag{2}$$

Accordingly, the block will remain at rest in this step. On the contrary, if $F^{(i)}_{spring}(t) > F^{(i)}_{s}(t)$ the block will start to move and the kinetic friction force is added to the spring force

$$F^{(i)}_{t}=F^{(i)}_{spring}-F^{(i)}_{k}. \tag{3}$$

The total force is similarly calculated, when the block is not at rest: $(\Delta x^{(i)}(t-\Delta t)\neq 0)$.

- *Simulation step* #2: *calculation of block displacements.* All blocks are visited, and based on forces $F^{(i)}_{t}$ calculated in simulation step #1, their displacements $\Delta x^{(i)}$ are calculated and stored. The displacement of the first block is $\Delta x^{(1)}=d_0$ which represents the constant drag step of the first block. For the rest of the blocks, $i=\overline{2,N}$, the displacement is calculated by using the equation of classical mechanics

$$\Delta x^{(i)}(t)=\Delta x^{(i)}(t-\Delta t)+A\,F^{(i)}(t)\Delta t^2, \tag{4}$$

where $A=1/2m$, m being the mass of a block.
- *Simulation step* #3: *application of restrictions.* For the calculated displacements, the block step limit $d_{\max}$ is applied which means that all displacement values greater than $d_{\max}$ are set to be $d_{\max}$.
- *Simulation step* #4: *updating block positions.* All blocks are visited following their ordinal numbers and their new positions are calculated by

$$x^{(i)}(t)=x^{(i)}(t-\Delta t)+\Delta x^{(i)}(t). \tag{5}$$

Here the only restriction is that a minimum distance $d_{\min}$ between blocks is always kept in order to ensure an accident-free dynamics.
- *Simulation step #5: data collection.* Stop times for the selected block are detected and stored in the output file. Stop time of a car is defined as the total time-length of consecutive simulation steps for which the displacement is zero. This is recorded at the time-moment where the car begins to move again. Car positions can also be stored at this step but this will result in a large amount of data. This feature is usually turned on for visualization purposes in case of small systems only.

Simulation steps #1–5 are repeated until enough data is collected for a proper statistical analysis.

According to the dynamics of the model there are some clear differences to previous car-following models [5]. The main difference is that a real driver is self-driven while this is clearly not the case in the spring-block system.

In our previous study [23] it was investigated how the position of a single block in the queue is influencing its stop-time distribution. From this study we learned that after a certain number of blocks (transient distance), their cumulative stop-time distribution converges to the same function. Therefore, in order to ensure that the right asymptotic behavior is studied, in the present study we simulate block chains longer than this transient distance, and the statistics for the last block in the row is investigated.

2.2. Realistic model parameters

The motion of the queue is simulated in discrete time-steps of length $\Delta t=1$. This fixes the unit for simulation time and gives us the possibility to handle easily the stochasticity in the equations of motion.

The length unit in the simulation is defined by the length of a single block $L=1$. This distance is not relevant for the studied statistics, but it has an importance in determining realistically some other relevant distances. In order to simulate the simplest dynamics without accidents, a minimum distance between blocks $d_{\min}=0.3$ is imposed. This distance is considered to be also the equilibrium length l_0 of the asymmetric springs. Taking into account that the length of a real car is around 4 m, this minimum distance corresponds to a 1.2 m minimum following distance. In the present simulations a step limit of $d_{\max}=1$ is also imposed for each car. This defines a speed limit for the blocks inside the row. It has to be noted that this speed limit value does not correspond to a usual speed limit applied in case of normal highway conditions. Here we have to take into account that in case of dense traffic conditions we are interested in a stronger speed-limiting factor that is governed by the average distance between cars. In our model this average distance goes up typically until 10 m. At such distances a speed limit of 36 km/h sounds to be a reasonable choice. By this selection, the real length of a simulation time-step will be $\Delta t_{real}=0.4$ s.

The motion of the queue is governed by the drag step (the movement of the first block) which is kept constant in time. In each unit of time the first block moves ahead in steps of length d_0 which fixes the velocity of the first car.

In our previous study [23] it was shown that except for high drag step values the average stop-time and the standard deviation of stop-times scales with the drag step following a $1/d_0$ functional dependence for any other model parameter values. In Fig. 2 this scaling is repeated for different disorder levels σ. In interpreting this scaling feature one has to keep in

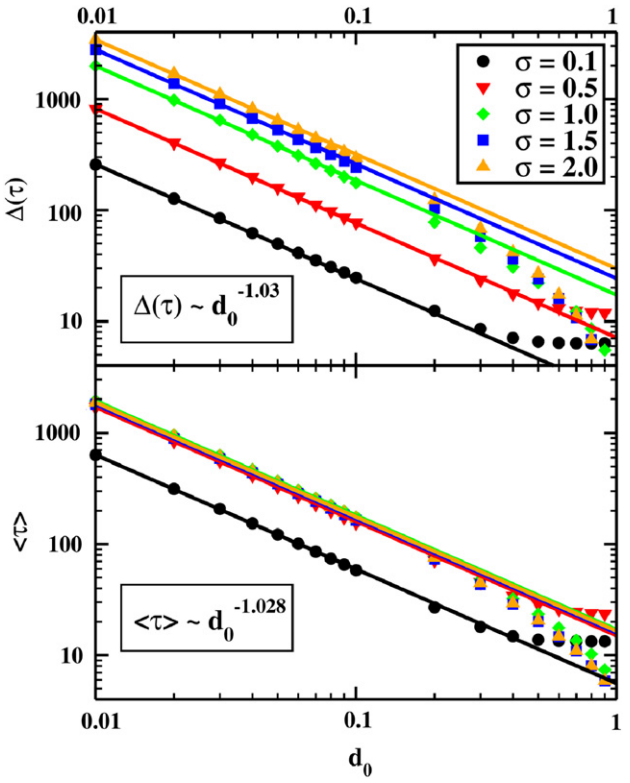

Fig. 2. Scaling of characteristic stop-times with the drag-step. Stop-time averages (bottom) and standard deviations (top) as a function of the drag steps. Results obtained from the statistics of 100 000 stop-times. Simulation results for different σ disorder levels are presented. The quantities in this figure are presented in simulation units.
Source: The simulation data is sourced from Ref. [23].

mind that in these simulations the time-step is kept constant. Thus, in order to reach the continuum limit, the drag step has to be reduced down to a value where this scaling is valid. Moreover, for small drag step values $d_0 \ll 1$ the scaling shows that the statistics of the systems' behavior is the same for any small drag velocities. In other words, in our later investigations this parameter value should be fixed to a small value (i.e. $d_0 = 0.05$ which means real velocities around 1.8 km/h) and then the results and conclusion will be valid for any drag velocities that are much smaller than the speed limit of the blocks. More evidence in this sense will be presented later, in the "Results" section of the article.

The motion of each block is governed by the total force acting on it. The force unit in the model has been selected by considering that all springs have the spring constant $k = 1$ and a unit elastic force acts on a block, when its distance to the block in front is $d_{\min} + 1$, expressed in simulation length units. With this force unit the mean value $\langle F_s \rangle$ and their standard deviation σ may be freely selected.

The constant A from Eq. (4) is chosen to be $A = 1$ which fixes the mass of blocks to $m = 0.5$ expressed in simulation units.

Therefore, in the following study the effect of the remaining three freely adjustable model parameters on the system dynamics will be investigated. These are the ratio f of the static and kinetic friction forces, the mean value of static friction force $\langle F_s \rangle$ and the disorder level σ.

3. Results

In real traffic conditions the data is usually collected by detectors located at fixed places. Accordingly, the number of passing cars in a given time interval (vehicle flow) is the most studied quantity. There are also other related and measured quantities like time headway, time clearance and time occupancy [5]. These quantities are, however, relevant for the whole system and they are not focusing on a single car in the row.

In our previous study [23] we turned the question around and we focused on what a driver stuck in the middle of a free or a congested traffic is experiencing. This can be quantified by the stop-time distribution $g(\tau)$ of the selected car in the row. This stop-time distribution describes the distribution of time intervals during which a given car is not moving. In other words, this distribution function $g(\tau)$ determines the probability density that the rest time of the car is τ. It also gives a hint on how predictable the traffic is for the driver. For instance, if the stop-time distribution has a narrow peak, drivers can

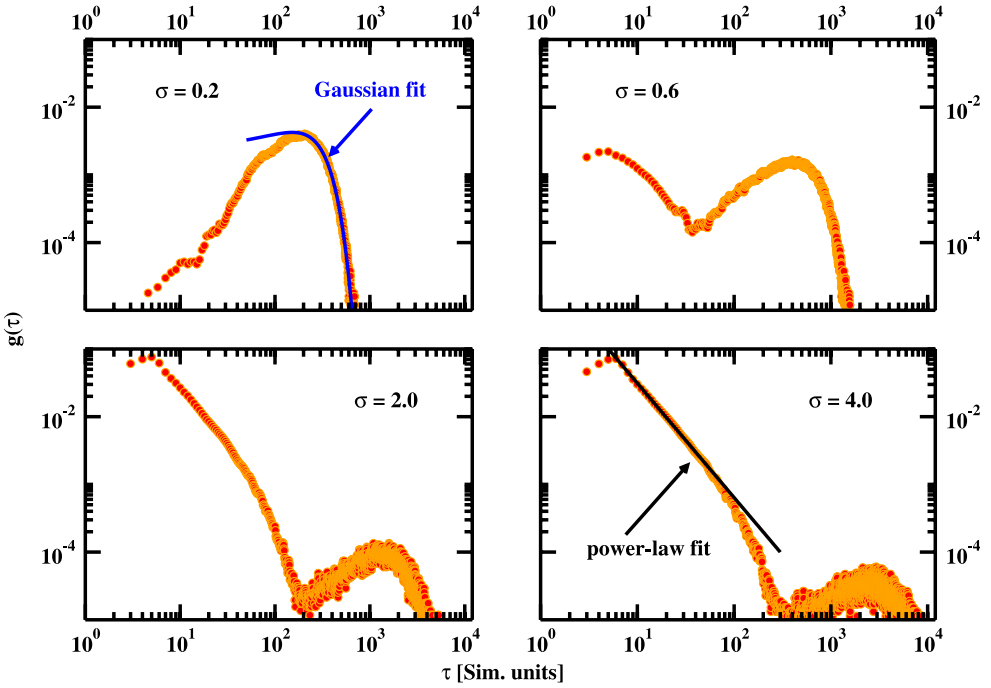

Fig. 3. Characteristic stop-time distributions. Normalized stop-time distributions for the last block in the chain for different disorder levels in the friction force σ. Results are obtained from a statistics of 100 000 stop-times.

predict how much time they are blocked in a given position. On the contrary, for a power-law type long tail distribution the waiting times are widely different and thus unpredictable.

Concerning the dynamics of the studied spring-block system interesting and non-trivial results have been reported in Ref. [23] by studying the average stop-time values and their standard deviation. Also, interesting results were obtained while studying the influence of the disorder level on the friction force values. It was observed that for a fixed mean static friction force value $\langle F_s \rangle$ at a certain disorder level ($\sigma \simeq 0.7$) there is a maximum in the average stop-time value [23]. This result suggested for example that in our simple traffic system there is a "worst" disorder level in driving attitudes (modeled by friction forces) for which the average stop-time of a block in the row is maximum.

3.1. Disorder induced phase transition

The disorder level in the system will be quantified in the following by dividing the stop-times standard deviation $\Delta(\tau)$ with the corresponding stop-time average $\langle \tau \rangle$. In such a manner, one single dimensionless parameter is obtained

$$r = \frac{\Delta(\tau)}{\langle \tau \rangle}, \tag{6}$$

which is appropriate as an order parameter. This order parameter will characterize the relative disorder in waiting times experienced by a driver. The simulations performed in the present work will focus on computing this order parameter as a function of the relevant f, $\langle F_s \rangle$ and σ parameters of the model.

As an example, in the following a case study will be performed for fixed $\langle F_s \rangle = 4$ and $f = 0.8$ parameter values. Stop-time distribution functions $g(\tau)$ are constructed from 100 000 simulated stop-times and they are plotted in Fig. 3 for different disorder levels σ. As is immediately observable, near the disorder level $\sigma = 0.6$ (second panel on Fig. 3) there are two peaks with the same magnitude in the stop-time distribution function. At lower disorder levels (first panel of Fig. 3) the first peak disappears and the stop-time distribution of long stop-times will be close to a normal distribution. This may be explained by assuming that in this region the motion of blocks is independent of each other and it is mainly influenced by friction forces generated randomly from a normal distribution. At higher disorder levels however (third and fourth panel of Fig. 3) the second part of the distribution function becomes less important. Moreover, the distribution is dominated by the first part which tends to a power-law type distribution suggesting correlated stops induced by collective motion of blocks and avalanche-like propagation of jams. Due to the continuous nature of the dynamics (molecular dynamics simulations and not cellular automata approach) quantifying the spatially propagating avalanches is complicated. Thus, the spatial propagation of these avalanches is not studied and the discussion is limited to the viewpoint of one block. The power-law trend in the observed stop-time distribution function suggests however a self-organized criticality as has already been reported in the

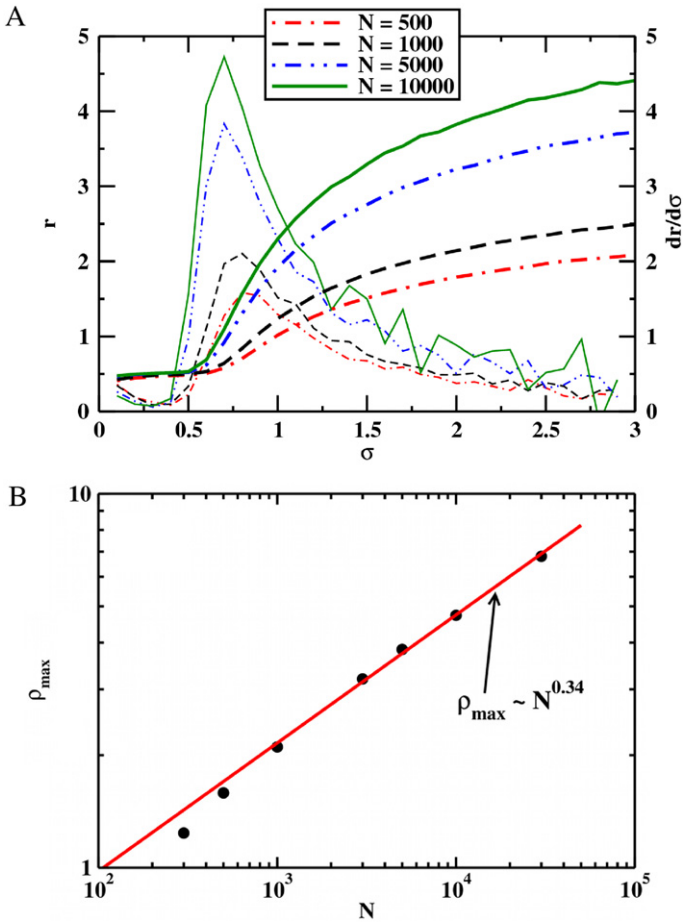

Fig. 4. Finite size effects. The order parameter r (thick lines) and its first derivative $\frac{dr}{d\sigma}$ (thin lines) as a function of the disorder level in the system σ are shown on panel A. Results for different system sizes N, are plotted. On panel B the maximum of the first order derivative $\rho_{\max}$ is plotted as a function of the system size. The parameter values for the simulations are the same as in Fig. 3 and all the quantities are expressed in simulation units.

two dimensional version of the spring-block model by Olami et al. [32]. The effects of disorder on these kinds of models have been studied by Janosi and Kertesz [33]. They have found that in a sandpile-type model disorder destroys criticality. Contrary with this result, in the present model criticality emerges as the disorder is increased. Here, it has to be noted that the power-law scaling of the stop-time distribution function stands only for one and a half orders of magnitude. Accordingly, we cannot be sure about the power-law nature of the distribution. However, for the purpose of the present work only the radical change in the stop-time distribution function is important, which is obvious in Fig. 3.

Let us visualize the above results using the order parameter r calculated from the same statistical data. Results as a function of the disorder level σ are plotted with continuous lines in Fig. 4(A). For investigating finite-size effects systems with different sizes are also considered. The graphs suggests that the order parameter has small values around $r \approx 0.5$ for low disorder levels ($\sigma \in [0.1, 0.7]$) and for higher disorder levels the order parameter is quickly reaching values greater than 1. Therefore, as a function of the disorder level in the system two different phases may be identified: the free flow phase and the self-organized congested flow (or jam) phase. The transition between these modes is realized through a disorder induced athermal phase transition. As the system size is increased steeper transition regimes are observable, in agreement with what one would expect for a second order phase transition. Plotting the derivative of the order parameter $\frac{dr}{d\sigma}$ for different system sizes (dashed lines on Fig. 4(A)) confirms the above conjecture. As plotted on Fig. 4(B) the maximum of the first order derivative $\rho_{\max}$ around $\sigma \approx 0.8$ is increasing monotonically with the system size, indicating that the first derivative of the order parameter diverges in case of infinite systems. This is a clear sign of a second order phase transition.

The motion of blocks in each phase of these two phases may be visualized by means of position–time diagrams. These are plotted in Fig. 5. On these graphs the position of each block is plotted along the horizontal axis at each simulation time-step considering the last 50 blocks of a row of 1000 units. In the bottom panel characteristic simulation results for systems with low disorder level (here with $\sigma = 0.2$) are presented. One will observe here that except for small perturbations, the spatiotemporal pattern of an almost continuous flow is outlined with short stop times that are not visible at the scale of the graph. On the contrary, in case of high disorder levels (here $\sigma = 2.0$ is chosen), the spatio-temporal pattern (top panel of

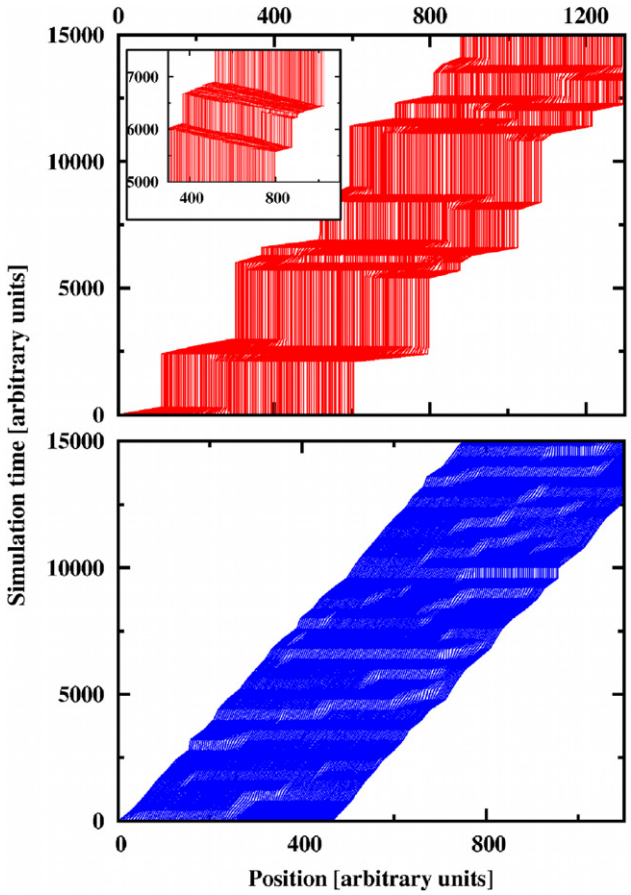

Fig. 5. Time diagrams for the traffic of the cars. Position of the last 50 cars (in a queue of 1000 cars) plotted as a function of time for two different σ values. The diagrams of block motions in the bottom panel indicate a continuous flow ($\sigma = 0.2$). The diagrams in the top panel indicate a congested flow phase ($\sigma = 2$). The inset panel shows the backwards propagating traffic waves by zooming into the 5000–7500 simulation time portion of the upper diagram.

Fig. 5) is stepwise with clearly visible stop-times on different time-scales and short headway periods between them. During this headway a self-organized shockwave-like motion of blocks may be detected. In order to visualize the waves a small part of the graph may be magnified. This magnified view is shown on the inset graph of Fig. 5. In agreement with observations and other traffic models the traffic waves of the spring-block model are backward propagating with propagation velocity $v_s = 18$ km/h which is close to the typical real traffic wave propagation velocity of 15–20 km/h [5].

Therefore, our simulation results suggest that the dynamics of the studied spring-block system viewed from the reference-frame of one block exhibits non-trivial, critical behavior. A disorder induced, athermal second order phase transition is observed, separating the independent block motions from a highly correlated avalanche-like collective motion.

3.2. Exploring the parameter space

Finally, using the order parameter defined and analyzed in the previous section the relevant parameter space of the spring-block traffic model is mapped. In six different color maps, on Fig. 6 the order parameter is represented as a function of the two main parameters of the model: the mean value of static friction force varied between $\langle F_s \rangle \in [0, 16]$ and the disorder level (varied between $\sigma \in [0.1, 3.0]$). Each created map is for a different kinetic/static friction force ratio taken in the interval $f \in [0.5, 1.0]$. The value of this f parameter is indicated near each figure. Each map contains 2430 data points and each point is calculated from a statistics of 100 000 simulated stop-times. The color coding has been calibrated in such a way that dark tones (blue in the colored version) represent order parameter values in the range $r \in [0, 0.7]$, and light grey tones (white to red and orange in the colored version) represent order parameter values in the range $r \in [0.7, 3.5]$.

In agreement with the previous case study performed for a single $\langle F_s \rangle$ value, on each parameter map the free flow and jam phases are clearly separated. For not too small $\langle F_s \rangle$ values the location of the phase separation point σ_{crit} (determined from the inflection points of the $r - \sigma$ curves) is well approximated by a linear dependence (see Fig. 7(A)):

$$\sigma_{crit}(\langle F_s \rangle) = \alpha(f)\langle F_s \rangle + \beta. \tag{7}$$

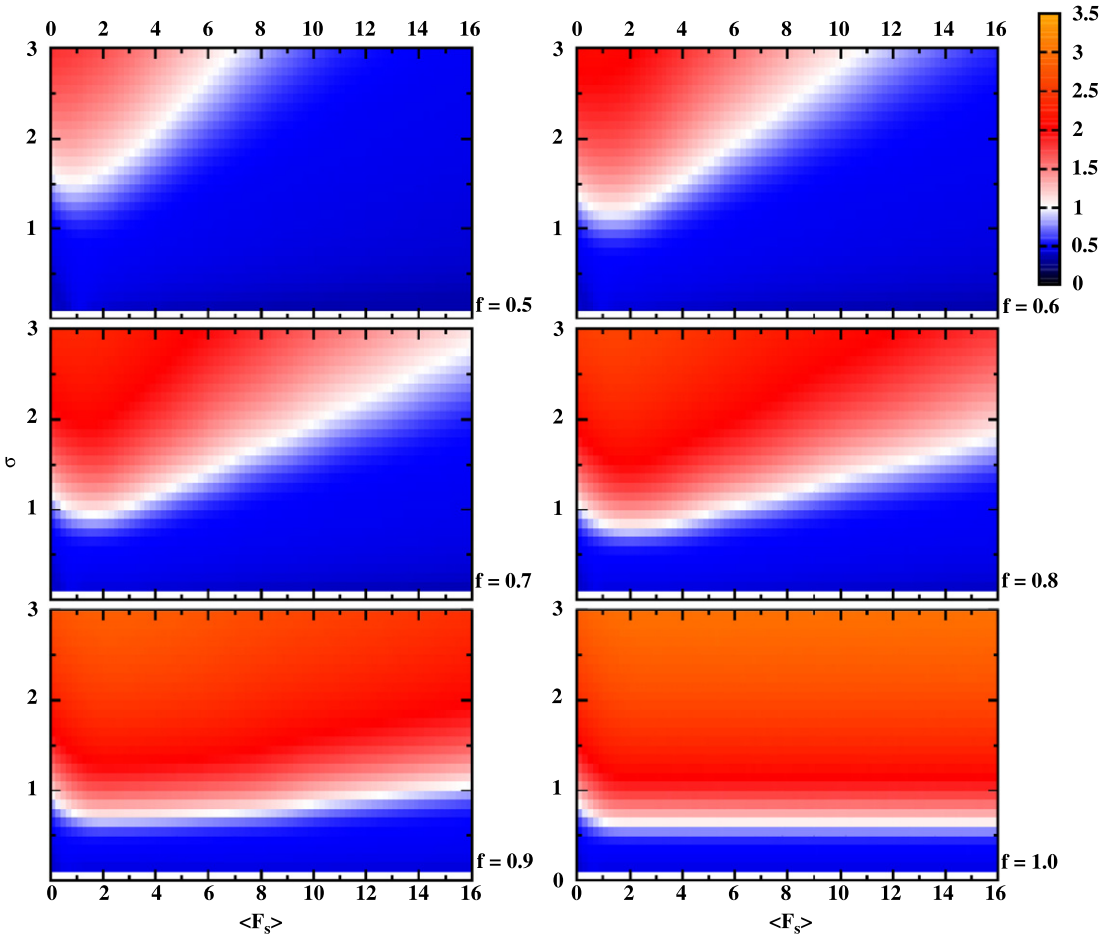

Fig. 6. Map of the parameter space. The color maps code the value of the order parameter, r, as a function of the $\langle F_s \rangle$ and σ parameters expressed in simulation units. Different panels correspond to different f ratios. (For interpretation of the references to colour in this figure legend, the reader is referred to the web version of this article.)

The slope α is decreasing as the f value increases up to 1.0 according to a quadratic trend (Fig. 7(B)). The relation (7) allows us to determine the disorder level σ_{crit} for any combination of the f and $\langle F_s \rangle$ parameter values.

4. Discussion and conclusions

Let us review now the experiment of Sugiyama et al. [18] from the viewpoint of the new modeling results. In their published video [20] vehicles are following each other on a circular track with the same imposed average velocity. After 10 min of circling, jams begin to emerge and propagate in the system. It is obvious, that after the long, boring and monotonic course, the drivers' attention reduces and the imperfections in their driving styles are increasing. In our spring-block approach this is equivalent to an increased average static friction value, $\langle F_s \rangle$. Assuming that all static friction values are changing proportionally the change in the average friction force value leads to a rescaling of the normal distribution's standard deviation $\sigma' = \sigma \frac{\langle F_s' \rangle}{\langle F_s \rangle}$. In order to have a more appropriate view on the behavior of the spring-block chain under such assumptions the order parameter map is reconstructed by using the relative standard deviation $\sigma_r = \frac{\sigma}{\langle F_s \rangle}$ which is constant for a proportional rescaling. On Fig. 8 we present results in such a sense for the $f = 0.8$ value. In contrast with Fig. 6, instead of the absolute standard deviation σ, the relative standard deviation σ_r is considered on the vertical axes. In this representation, the increase in the erratic components of the driving styles is equivalent with a horizontal displacement of the system's characteristic point to the right (i.e. from point A to B). As indicated on Fig. 8, by such displacements it is possible to have a transition from the free flow phase (blue region) to the jammed phase (red region). Accordingly, our model system confirms that the reduced attention of the drivers may induce the emergence of phantom traffic jams. The other way to have a transition from the free flow phase to the jammed flow phase (i.e. from point A to C) is through an increased disorder in driving imperfections which may be induced by some unexpected traffic conditions.

It is important also to comment on the influence of the drag velocities or drag steps, d_0, on the observed statistics. Based on the simple scaling relation for the average value of the stop-times and their standard deviation as a function of the

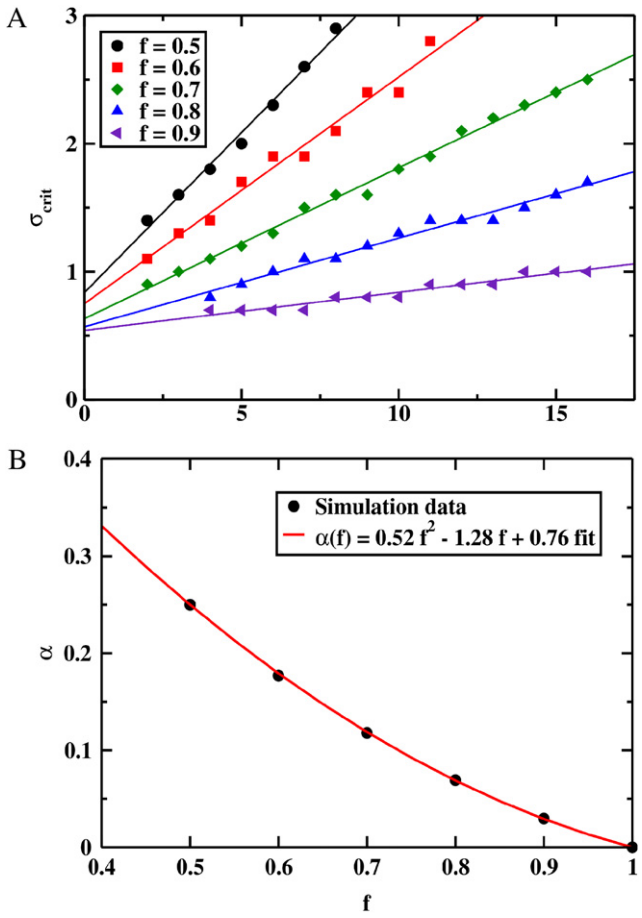

Fig. 7. Location of the phase boundaries. Figure (A) presents the critical disorder level as a function of the $\langle F_s \rangle$ static friction value. Figure (B) plots the slope α of the $\sigma_{crit} - \langle F_s \rangle$ lines as a function of the kinetic to static friction force ratio, f. The quantities on both panels are expressed in simulation units.

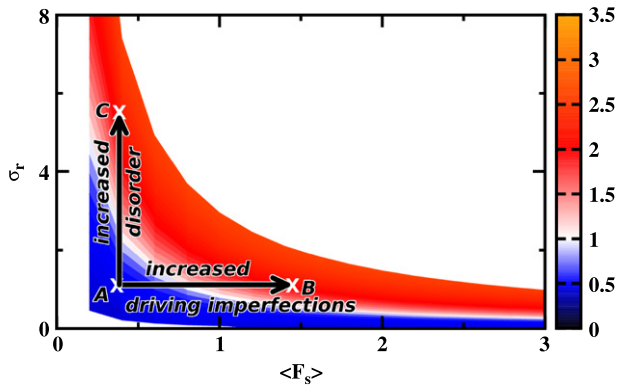

Fig. 8. Effect of driving imperfections and differences in driving attitudes. The color code indicates the order parameter value as a function of the $\sigma_r = \frac{\sigma}{\langle F_s \rangle}$ relative standard deviation and $\langle F_s \rangle$ values expressed in simulation units. Increased driving imperfections or disorder in driving attitudes drives the system from a continuous flow phase to a congested traffic phase. Phantom traffic jams are thus a result of either increased disorder in driving attitudes or increased imperfections in driving style of drivers. (For interpretation of the references to colour in this figure legend, the reader is referred to the web version of this article.)

drag step (Fig. 2), we already emphasized that for small drag step values $d_0 \ll 1$ the system's behavior is re-scalable. This presumption may be confirmed by performing a series of simulations where the relative standard deviation σ_r and the kinetic/static friction force ratio f is kept constant. Fig. 9 shows results in such a sense. Here the order parameter and its first derivative is plotted as a function of $\langle F_s \rangle$ for different drag step values, d_0. From the obtained curves it is immediately observable that in the small drag step limit the critical point separating the two phases is not influenced by the chosen drag

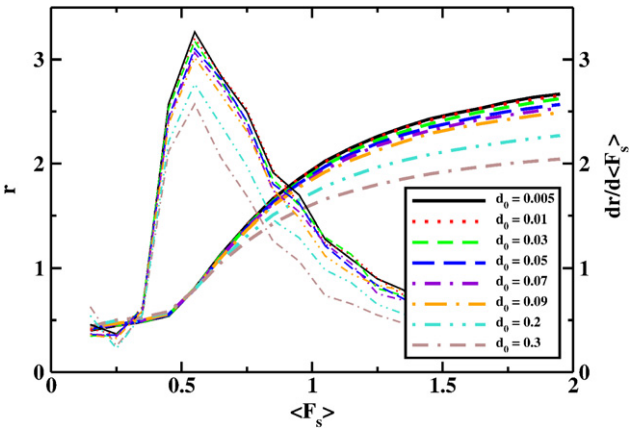

Fig. 9. Effect of drag velocity on the obtained phase transition. The order parameter (continuous lines) and its first derivative (dashed lines) are plotted as a function of the static friction for different d_0 drag-step values. All quantities are expressed in simulation units. The results confirm that the obtained phases are the same independently of the chosen drag-step values.

step value. The phases that appear for different drag velocities are thus not influenced by the chosen drag velocity, assuming that this value is small. The obtained results are thus easily generalizable for all small drag velocity values.

In conclusion, a simple one-dimensional asymmetric spring-block chain inspired from the early earthquake models has been adapted to model the idealized single-lane highway traffic. The model has three free parameters, and a thorough mapping of the parameter space indicates two clearly distinguishable phases and a rich collective behavior. A disorder induced second order phase transition has been observed, separating the free flow phase from the congested flow phase which is dominated by a highly correlated avalanche-like collective motion. Through these computer simulation studies it was confirmed that the emergence of phantom traffic jams characterized by continuous formation and propagation of jamitons [14,17] may be induced by an overall reduction of drivers' attention. Another effect that can lead to the appearance of phantom traffic jams is the increased differences in imperfect driving attitudes.

Acknowledgments

This work was supported by the Romanian National Research Council (CNCS-UEFISCSU), project number PN II-RU PD_404/2010. The funders had no role in study design, data collection and analysis, decision to publish, or preparation of the manuscript.

References

[1] R. Burridge, L. Knopoff, Model and theoretical seismicity, Bull. Seismol. Soc. Amer. 57 (3) (1967) 341–371.
[2] B. Gutenberg, C.F. Richter, Magnitude and energy of earthquakes, Ann. Geophys. 9 (1956) 1–15.
[3] G. Mate, Z. Neda, J. Benedek, Spring-block model reveals region-like structures, PLOS One 6 (8) (2011) e16518/1-8. http://dx.doi.org/10.1371/journal.pone.0016518.
[4] T. Nagatani, The physics of traffic jams, Rep. Progr. Phys. 65 (9) (2002) 1331–1386. http://dx.doi.org/10.1088/0034-4885/65/9/203.
[5] D. Helbing, Traffic and related self-driven many-particle systems, Rev. Modern Phys. 73 (4) (2001) 1067–1141. http://dx.doi.org/10.1103/RevModPhys.73.1067.
[6] B. Greenshields, A study of highway capacity, in: Proceedings of the 14th Annual Meeting of the Highway Research Board 14, 1935, pp. 448–477.
[7] B. Kerner, H. Rehborn, Experimental properties of phase transitions in traffic flow, Phys. Rev. Lett. 79 (20) (1997) 4030–4033. http://dx.doi.org/10.1103/PhysRevLett.79.4030.
[8] J. Banks, Review of empirical research on congested freeway flow, in: Traffic Flow Theory and Highway Capacity 2002: Highway Operations, Capacity, and Traffic Control, No. 1802 in Transport. Res. Rec., 2002, pp. 225–232, 81st Annual Meeting of the Transportation-Research-Board, WASHINGTON, D.C., JAN, 2002.
[9] M. Atluri, M. Chowdhury, N. Kanhere, R. Fries, W. Sarasua, J. Ogle, Development of a sensor system for traffic data collection, J. Adv. Transp. 43 (1) (2009) 1–20.
[10] E. Sifuentes, O. Casas, R. Pallas-Areny, Wireless magnetic sensor node for vehicle detection with optical wake-up, IEEE Sens. J. 11 (8) (2011) 1669–1676. http://dx.doi.org/10.1109/JSEN.2010.2103937.
[11] D. Chowdhury, L. Santen, A. Schadschneider, Statistical physics of vehicular traffic and some related systems, Phys. Rep. 329 (4–6) (2000) 199–329. http://dx.doi.org/10.1016/S0370-1573(99)00117-9.
[12] S. Maerivoet, B. De Moor, Cellular automata models of road traffic, Phys. Rep. 419 (1) (2005) 1–64. http://dx.doi.org/10.1016/j.physrep.2005.08.005.
[13] S. Darbha, K.R. Rajagopal, V. Tyagi, A review of mathematical models for the flow of traffic and some recent results, Nonlinear Anal. TMA 69 (3) (2008) 950–970. http://dx.doi.org/10.1016/j.na.2008.02.123.
[14] R. Mahnke, J. Kaupuzs, I. Lubashevsky, Probabilistic description of traffic flow, Phys. Rep. 408 (1–2) (2005) 1–130. http://dx.doi.org/10.1016/j.physrep.2004.12.001.
[15] M. Treiber, A. Kesting, D. Helbing, Delays, inaccuracies and anticipation in microscopic traffic models, Physica A 360 (2006) 71–88.
[16] M. Schönhof, D. Helbing, Empirical features of congested traffic state and their implications for traffic modeling, Transp. Sci. 41 (2007) 135–166.
[17] M. Schonhof, D. Helbing, Criticism of three-phase traffic theory, Transp. Res. B-Meth. 43 (2009) 784–797.
[18] Y. Sugiyama, M. Fukui, M. Kikuchi, K. Hasebe, A. Nakayama, K. Nishinari, S.-i. Tadaki, S. Yukawa, Traffic jams without bottlenecks — experimental evidence for the physical mechanism of the formation of a jam, New J. Phys. 10 (2008) 033001. http://dx.doi.org/10.1088/1367-2630/10/3/033001.

[19] A. Nakayama, M. Fukui, M. Kikuchi, K. Hasebe, K. Nishinari, Y. Sugiyama, S.-i. Tadaki, S. Yukawa, Metastability in the formation of an experimental traffic jam, New J. Phys. 11 (2009) 083025. http://dx.doi.org/10.1088/1367-2630/11/8/083025.
[20] Y. Sugiyama, M. Fukui, M. Kikuchi, K. Hasebe, A. Nakayama, K. Nishinari, S.-i. Tadaki, S. Yukawa, Shockwave traffic jams recreated for first time (MAR 2008) [cited 2011]. http://www.youtube.com/watch?v=Suugn-p5C1M.
[21] M.R. Flynn, A.R. Kasimov, J.-C. Nave, R.R. Rosales, B. Seibold, Self-sustained nonlinear waves in traffic flow, Phys. Rev. E 79 (2009) 056113.
[22] K. Kovacs, Z. Neda, Disorder-driven phase transition in a spring-block type magnetization model, Phys. Lett. A 361 (1–2) (2007) 18–23. http://dx.doi.org/10.1016/j.physleta.2006.08.086.
[23] F. Jarai-Szabo, B. Sandor, Z. Neda, Spring-block model for a single-lane highway traffic, Cent. Eur. J. Phys. 9 (4) (2011) 1002–1009. http://dx.doi.org/10.2478/s11534-011-0007-6.
[24] K. Leung, Z. Neda, Pattern formation and selection in quasistatic fracture, Phys. Rev. Lett. 85 (3) (2000) 662–665. http://dx.doi.org/10.1103/PhysRevLett.85.662.
[25] K. Leung, L. Jozsa, M. Ravasz, Z. Neda, Pattern formation — spiral cracks without twisting, Nature 410 (6825) (2001) 166. http://dx.doi.org/10.1038/35065517.
[26] F. Jarai-Szabo, S. Astilean, Z. Neda, Understanding self-assembled nanosphere patterns, Chem. Phys. Lett. 408 (4–6) (2005) 241–246. http://dx.doi.org/10.1016/j.cplett.2005.04.051.
[27] F. Jarai-Szabo, Z. Neda, S. Astilean, C. Farcau, A. Kuttesch, Shake-induced order in nanosphere systems, Eur. Phys. J. E 23 (2) (2007) 153–159. http://dx.doi.org/10.1140/epje/i2006-10194-9.
[28] F. Jarai-Szabo, E.-A. Horvat, R. Vajtai, Z. Neda, Spring-block approach for nanobristle patterns, Chem. Phys. Lett. 511 (4–6) (2011) 378–383. http://dx.doi.org/10.1016/j.cplett.2011.06.068.
[29] A. Kesting, M. Treiber, How reaction time, update time, and adaptation time influence the stability of traffic flow, Comput. Aided Civ. Inf. 23 (2008) 125–137.
[30] R. Barlovic, L. Santen, A. Schadschneider, M. Schreckenberg, Metastable states in cellular automata for traffic flow, Eur. Phys. J. B 5 (3) (1998) 793–800.
[31] K. Nagel, M. Schreckenberg, A cellular automaton model for freeway traffic, J. Phys. I 2 (12) (1992) 2221–2229.
[32] Z. Olami, H.J.S. Feder, K. Christensen, Self-organized criticality in a continuous, nonconservative cellular automaton modeling earthquakes, Phys. Rev. Lett. 68 (1992) 1244–1247. http://dx.doi.org/10.1103/PhysRevLett.68.1244.
[33] I.M. Janosi, J. Kertesz, Self-organized criticality with and without conservation, Physica A 200 (1–4) (1993) 179–188. http://dx.doi.org/10.1016/0378-4371(93)90516-7.